JACS
JOURNAL OF THE AMERICAN CHEMICAL SOCIETY

ARTICLE

pubs.acs.org/JACS

New SmCG Phases in a Hydrogen-Bonded Bent-Core Liquid Crystal Featuring a Branched Siloxane Terminal Group

Wei-Hong Chen,[†] Wei-Tsung Chuang,[*,‡] U-Ser Jeng,[‡] Hwo-Shuenn Sheu,[‡] and Hong-Cheu Lin[*,†]

[†]Department of Materials Science and Engineering, National Chiao Tung University, Hsinchu, 30049, Taiwan

[‡]National Synchrotron Radiation Research Center, Hsinchu, 30076, Taiwan

Supporting Information

ABSTRACT: In this study, we synthesized three analogous bent-core molecules, a hydrogen-bonded complex and a covalent-bonded compound with branched siloxane units (**H−SiO** and **C−SiO**, respectively) and a hydrogen-bonded complex with an alkyl unit (**H−Alk**), and investigated the effects of the hydrogen bonding and branched siloxane terminal units on their mesomorphic properties. The covalent-bonded compound **C−SiO** and the hydrogen-bonded complex **H−Alk** exhibited typical SmCP phases; in contrast, the hydrogen-bonded complex **H−SiO** exhibited a series of general tilt smectic (SmCG) phases with highly ordered layer structures (i.e., $SmCG_2P_F$−$USmCG_2P_A$−$SmCG_2P_F$−$SmCGP_F$ upon cooling). During the SmCG-type phase transition process, a 2D-modulated ribbon structure transferred into highly ordered layers via undulated layers, as the hydrogen-bonding strength increased with reduced temperatures. As the SmCG domains were aligned under dc electric fields, a gradual decrease in the leaning angle from ca. 60° to 50° (while the tilt angle kept at ca. 31°) could be determined by in situ wide-angle X-ray scattering (WAXS). Combined with Fourier transform infrared and Raman spectroscopic data, our results suggest that the change in the leaning angle was governed by the competition of the hydrogen bonds and microsegregation of siloxane units within the bilayer structure of the hydrogen-bonded complex **H−SiO**. In addition, the ferroelectric−(antiferroelectric)−ferroelectric transitions proven by the switching current responses in the SmCG-type phases of **H−SiO** reveal that the polar switching occurred through collective rotations around the long axis of **H−SiO**. Therefore, novel SmCG phases with a series of highly ordered 2D-structures were induced by the effects of the hydrogen bonding and branched terminal siloxane unit in the bent-core hydrogen-bonded LC complex **H−SiO**.

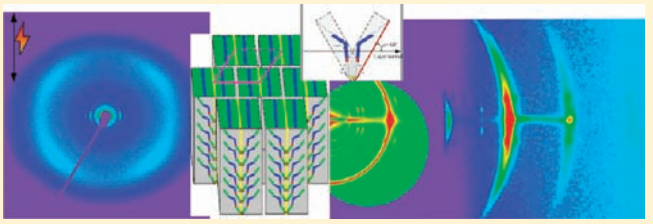

INTRODUCTION

Bent-core liquid crystals (LCs) have received great attention since the discovery, by Niori et al.,[1] of their special electro-optical properties, such as polar switching behaviors, spontaneous polarized capabilities, and nonlinear optics.[2] Several studies have been made into the effects of the configuration of the bent-core molecules, including the zenithal constituent, the shape of the rigid core, the lengths of the flexible chains, and the role of substituents at selective positions of a rigid core, on the properties of the LCs.[2] Those effects strongly influence the mesophases of the bent-core molecules, resulting in eight main mesophases, denoted B1−B8,[2] with smectic, columnar, or three-dimensional orders having been discovered to date. Depending upon the direction of polarization in the continuous layers and the molecular tilt angle with respect to the layer normal, the bent-core molecules spontaneously exhibit polar and chiral layers, leading to SmCP phases (B2) having four layer-type structures with a ferroelectric or antiferroelectric state, the homochiral SmC_SP_F and SmC_aP_A and racemic SmC_aP_F and SmC_SP_A phases.[2] As a result of the splay of polarization in smectic layers,[3] modulation induces the breaking layers or ribbons to undergo long-range ordering in the two-dimensional 2D lattices of oblique (Col_{ob}) and rectangular (Col_r) phases.[2] These modulated smectic phases have also displayed antiferroelectric switching ($Col_{ob}P_A$, Col_rP_A)[4] and ferroelectric switching columnar phases ($Col_{ob}P_{FE}$, Col_rP_{FE}).[5]

In addition to the typical SmC and modulated SmC phases, bent-core molecules have the potential to display a rarely observed related phase: a double-tilted smectic phase having a chiral C_1 symmetry configuration, assigned to a SmCG phase, as proposed by de Gennes et al.[6] Two tilted angles are defined with respect to the layer normal: the tilt of the molecular plane (clinicity) and the tilt of the molecular kink direction (leaning). This double-tilt conformation gives rise to syn-leaning and anti-leaning structures in addition to syn-clinic and anti-clinic configurations in the SmC phase. On the basis of these conformational varieties, eight different orientations are possible for molecular packing in the SmCG phase;[7] nevertheless, few experimental studies have been reported regarding the realization of the SmCG phase in bent-core molecules.

Most modulated bilayer structures composed of asymmetric bent-core molecules have been assumed to feature a double tilt $SmCG_2$ phase;[8,9] nevertheless, unambiguous evidence for the

Received: June 22, 2011
Published: August 26, 2011

leaning angle has been rare. The $SmCG_2$ phase was suggested to relate to the deflection of the molecular mass center in consecutive layers in symmetric and asymmetric molecular structures of the bent-shaped molecules.[9c] Recently, a series of phase transitions $Sm\tilde{C}G_2-SmCG_2-SmC$ was examined through X-ray diffraction and construction of electron density maps in an attempt to elucidate the formation of modulation for the $Sm\tilde{C}G_2$ phase;[9b] even so, the origin of the SmCG-phase transitions was not fully addressed.

Providing an interesting approach toward generating novel and creative materials through supramolecular chemistry, hydrogen-bonded bent-core LCs composed of nonmesomorphic small molecules is a leading topic in the field of LCs because of their potential application in biomaterials[10] and electro-optical devices.[11] Supramolecular interactions between functionalized proton donors (H-donor) and proton acceptors (H-acceptor) bearing complementary binding sites can provide new complexes exhibiting mesomorphic structures. A fundamental understanding of supramolecular self-assembling LC systems will be necessary for their future scientific and technological development. The nature of the pendant groups on the bent-cores of hydrogen-bonded bent-core LCs can affect their electric and optical behavior.[12] Lin et al. have studied how the mesophasic type is influenced by (i) the hydrogen-bonded site of the core, (ii) the total number of aromatic units in the hydrogen-bonded core, and (iii) the presence percentages of hydrogen and covalent bonds in hydrogen-bonded side-chain copolymers.[13] Tschierske et al. studied the properties of bent-core structures containing siloxane units at one or both ends of the flexible alkyl chain termini.[14] They suggested that the siloxane units segregate into divided sublayers at the interfaces between adjacent layers; this microsegregation alters the phase characterization of the bent-core molecules. From the viewpoint of molecular design, the hydrogen-bonded bent-core molecules combined with the siloxane units might provide interesting supramolecular LC structures; to the best of our knowledge, however, such systems have not been investigated previously.

In this study, we synthesized a new hydrogen-bonded complex and a covalent-bonded compound with branched siloxane units (**H−SiO** and **C−SiO**, respectively) and a hydrogen-bonded complex lacking siloxane units (**H−Alk**) to explore the effects of both hydrogen bonds and branched siloxane units. The complex of hydrogen-bonded bent-core molecules with the branched siloxane unit exhibited a series of SmCG-type phase transitions. We determined the leaning angles of these SmCG-type phases using synchrotron-based in situ small-angle X-ray scattering (SAXS) and wide-angle X-ray scattering (WAXS) measurements under dc electric fields. To probe the origin of the SmCG-type phase transitions, we examined the relationship between the variation in leaning angle and the interplay between the competition of hydrogen bonds and microsegregation of the siloxane units. Herein, we provide a possible explanation for the rare SmCG-type phase transitions, based on the results obtained from in situ X-ray scattering and Fourier transform infrared (FTIR) and Raman spectra.

EXPERIMENTAL SECTION

Synthesis and Sample Preparation. Three structurally similar molecules were synthesized; their molecular structures are provided in Scheme 1. Hydrosilylation of the olefinic compounds was performed using 1,1,1,3,5,5,5-heptamethyltrisiloxane in the presence of Karstedt's catalyst.[15] The hydrogen-bonded complexes **H−SiO** and **H−Alk** were prepared by mixing appropriate molar ratios (1:1) of the H-donor (**3SiA** and **A12**, respectively) and the H-acceptor **VPy** in THF solution at 40 °C to obtain the self-assembled asymmetric bent-core complexes. Synthetic procedures for all of the compounds are provided in the Supporting Information. The homeotropic aligned samples of the bent-core molecules were obtained by heating small amounts of compounds from the isotropic state with a very slow cooling rate on a glass substrate treated with a commercially available homeotropic agent, for the 2D-XRD patterns. Evidence for hydrogen bonding in these asymmetric heterodimers was obtained using FTIR spectroscopy (Figure S1). A similarly structured, covalent-bonded bent-core molecule featuring the same siloxane unit (**C−SiO**) was synthesized as a control. The phase transition temperatures and enthalpies of the three systems, obtained using differential scanning calorimetry (DSC; Figure S2), are listed in Table 1.

Characterization Methods. ^{1}H NMR spectra were recorded using a Varian Unity 300 MHz spectrometer, with DMSO-d_6 and $CDCl_3$ as solvents. Mass spectral data were obtained using a Micromass TRIO-2000 GC/MS system. Elemental analyses were performed using a Heraeus CHN-OS RAPID elemental analyzer. Mesophasic textures were characterized using a Leica DMLP polarizing optical microscope equipped with a Linkam hot stage. FTIR spectra were recorded using a Thermo Nicolet Nexus 6700 instrument. Raman spectroscopy was performed using a He−Ne 633 laser source.

Synchrotron-based small-angle and wide-angle X-ray scattering measurements in conjunction with grazing-incidence scattering (SAXS/GISAXS and WAXS/GIWAXS, respectively) were performed at the BL23A SAXS and BL01C2 XRD endstations, respectively, of the National Synchrotron Radiation Research Center, Hsinchu, Taiwan.[16] With the marCCD165 detector used for SAXS and the mar345 image plate for WAXS, typical scattering patterns were collected from at least 60 to 300 s to obtain sufficient scattering intensities. The beam diameter of the 10 keV beam (λ = 0.124 nm^{-1}) was 0.5 mm. The scattering vectors ($q = 4\pi/\lambda \sin\theta$; with scattering angle 2θ) for SAXS and WAXS were calibrated using two standard samples of silver behenate and silicon. The three synthesized systems were subjected to homeotropical alignment on a glass substrate for the GISAXS and GIWAXS measurements. With electric-field alignment, the sample cells for in situ X-ray scattering measurement consisted of two stainless-steel electrodes having a thickness of 1 mm separated by a controlled gap of 0.6 mm (see Figure S3). This electrode configuration was held in the modified Linkam hot stage. Samples were heated above the isotropic temperature within the electrodes and held in place by capillary forces. A dc electric field of 200 V was applied across the electrodes while in the isotropic phase; the sample was then cooled to within the given temperature region. The incident X-rays were aligned normal to the direction of the applied electric field. Two sample alignments of the surface and electric field, combined with the X-ray scattering measurements, provided views parallel and perpendicular to the bending plane of bent-core molecules, respectively. When the molecules are well aligned, the former provided the tilt angle from the diffuse scattering halo, and the latter provided the leaning angle of the SmCG phase.

The electro-optical properties were determined in commercially available indium tin oxide (ITO) cells (mesostate; thickness, 7.5 μm; active area, 1 cm^2) featuring rubbed polyimide alignment coatings (parallel rubbing direction). A digital oscilloscope (Tektronix TDS-3012B) was used in these measurements; a high-power amplifier connected to a function generator (GW model GFG-813) with a dc power supply (Keithley 2400) was used in the dc field experiments. During electro-optical measurements, the modulation of the texture under the applied electric field was monitored using polarizing optical microscopy (POM).

RESULTS AND DISCUSSION

To study the effects of the hydrogen bonds and branched siloxane units on the mesomorphic properties of LC molecules,

Scheme 1. Chemical Structures of the Hydrogen-Bonded Complex and Covalent-Bonded Compound with Siloxane Units (H−SiO and C−SiO, Respectively) and the Hydrogen-Bonded Complex Lacking a Siloxane Unit (H−Alk)

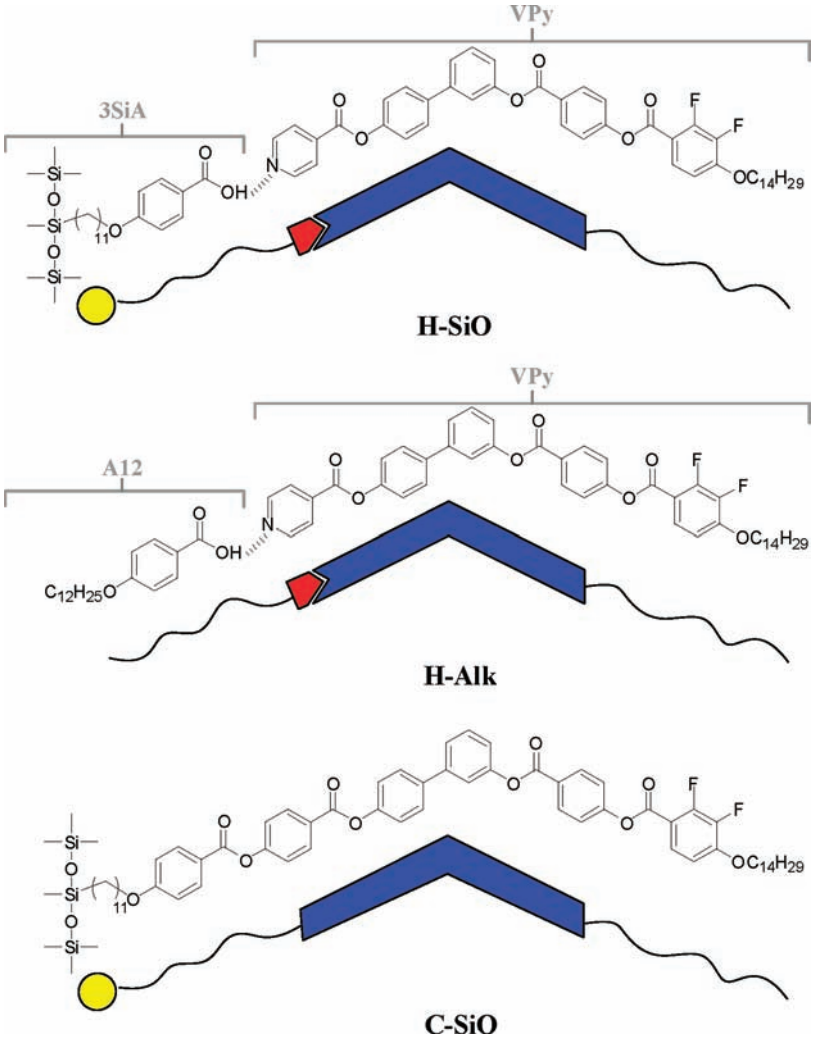

Table 1. Phase Transition Temperatures and Enthalpies of the Hydrogen-Bonded Complex and Covalent-Bonded Compound with Siloxane Units (H−SiO and C−SiO, Respectively) and the Hydrogen-Bonded Complex Lacking Siloxane Units (H−Alk)[a]

compound	phase transition temperature (°C) and enthalpy (kJ/mol)
H−SiO	Cr 75.9[22.8],[b] $SmCGP_F$ 86.0, $SmCG_2P_F$ 97.0, $USmCG_2P_A$ 115.0, $Sm\tilde{C}G_2P_F$ 132.1 [28.6],[b] Iso
H−Alk	Cr 96.4 [19.5],[b] $SmCP_A$ 128.6 [30.9],[b] Iso
C−SiO	Cr 49.3 [10.7],[b] $SmCP_F$ 172.5 [29.7],[b] Iso

[a] Mesophasic types and transition temperatures were observed using XRD and switching current measurements in terms of changes in polar switching behavior. [b] Phase transitions were measured from the second cooling scan of DSC (cooling rate: 5 °C min^{-1}).

we used POM and DSC to investigate the compound with siloxane units (**H−SiO** and **C−SiO**, respectively) and a hydrogen-bonded complex lacking a siloxane unit (**H−Alk**). In contrast to the mesophasic ranges of the hydrogen-bonded complexes with and without siloxane units (56.2 and 32.2 °C for **H−SiO** and **H−Alk**, respectively), the bent-core covalent-bonded compound **C−SiO** exhibited a broader LC phase range (ca. 123.2 °C) because the covalent-bonded structure bearing a siloxane unit stabilized the LC phase[2a,14] (see Table 1). POM images revealed characteristic fan textures for **H−Alk**, **C−SiO**, and **H−SiO** (Figures 1−3, respectively).

Substrate-Oriented SmCG-type Phases. To investigate the mesophasic types of these analogous bent-core molecules, well-aligned samples were prepared via homeotropic alignment technique (as described in the Experimental Section) to observe the side-view of the molecular arrangements by GISAXS/GIWAXS patterns. In Figure 1a, the GIWAXS pattern of the hydrogen-bonded complex **H−Alk** reveals layer-like reflections on meridian, yielding a layer spacing (d_{layer}) of 5.2 nm that is smaller than the theoretical molecular length of the complex **H−Alk** (L = 6.3 nm), indicating the tilted arrangement of a smectic structure (SmC phase). The diffuse scattering halo at a value of q of approximately 14 nm^{-1} (d = 0.45 nm) represents the mean distance between liquid-like alkyl chains. Two azimuthal maxima among the halo located out of the equator reveal a tilt angle ω of approximately 30°

(consistent with the tilt angle of 34° calculated using the equation $\cos \omega = d_{layer}/L$) for the long molecular axes with respect to the layer normal. In Figure 1b, the POM image displays the weak birefringence texture of the SmC phase in the hydrogen-bonded complex **H**−**Alk**. For the covalent-bonded compound **C**−**SiO**, the layer-like reflections, observed as Deby−Scherrer rings, in Figure 2a reveal a layer spacing of 6.8 nm, slightly smaller than the molecular length of 7.1 nm, suggesting a small tilted angle in the SmC phase. The SmC phase of the covalent-bonded compound **C**−**SiO**, characterized by high viscoelasticity, was negligibly aligned by the surface and electric-field alignments, leading to a powder-like form. Figure 2b displays the high birefringence in the fan-like texture of the covalent-bonded compound **C**−**SiO**.

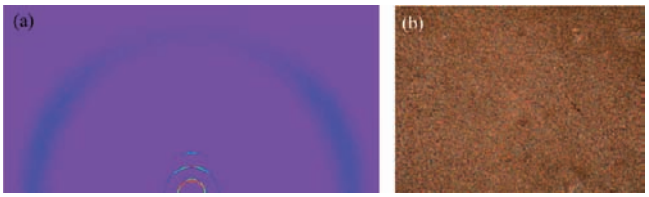

Figure 1. (a) GIWAXS pattern and (b) POM image of the surface-aligned sample of the hydrogen-bonded complex **H**−**Alk** at 110 °C.

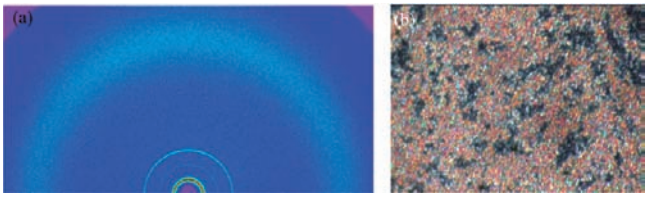

Figure 2. (a) GIWAXS pattern and (b) POM image of the surface-aligned sample of the covalent-bonded compound **C**−**SiO** at 100 °C.

Because of a large structure size in the hydrogen-bonded complex **H**−**SiO**, we present combined GISAXS and GIWAXS patterns to show the complete reflections in the full q scale. Figure 3a−d displays the combined GISAXS and GIWAXS patterns at representative temperatures, after cooling from the isotropic temperature (140 °C), for the surface-aligned sample of the hydrogen-bonded complex **H**−**SiO**; POM images are provided as insets. Figure 3a observed at 130 °C is the highly ordered reflections located along the meridional and off-meridional directions of the GISAXS/GIWAXS patterns, indicating a highly ordered structure. Using an oblique 2D lattice, with the two lattice parameters a (=19.1 nm) and c (=12.9 nm) and an oblique angle β (96°), we can index all reflections in Figure 3a. The d-spacing of (01) (12.8 nm) corresponds to a bilayer spacing of the LC domains of the hydrogen-bonded complex **H**−**SiO** (in which the molecular length is ca. 7.2 nm). Assuming an average distance of 0.5 nm between molecular planes, the bilayer spacing, and a density of 1.0 g cm^{-3} for **H**−**SiO**, we have further estimated that each cross section of the ribbon unit shown in Figure 3a may consist of ca. 70 bent-core molecules. This large ribbon dimension is less commonly observed in a bent-core LC.

As the temperature decreased to 110 °C (Figure 3b), the (20) reflection at the equatorial direction and some higher-order diffractions at the off-meridian direction disappeared, while the (11) and (−11) reflections moved toward to the meridian. These changes signify merging of ordered ribbons into undulated bilayers. Further cooling to 95 °C, the diminishing (11) and (−11) reflections were nearly absorbed into the (01) reflection spot. At 85 °C, approaching the LC phase border, signature reflections of the bilayer structure were largely gone, leaving only characteristic reflections from lamellae of characteristic

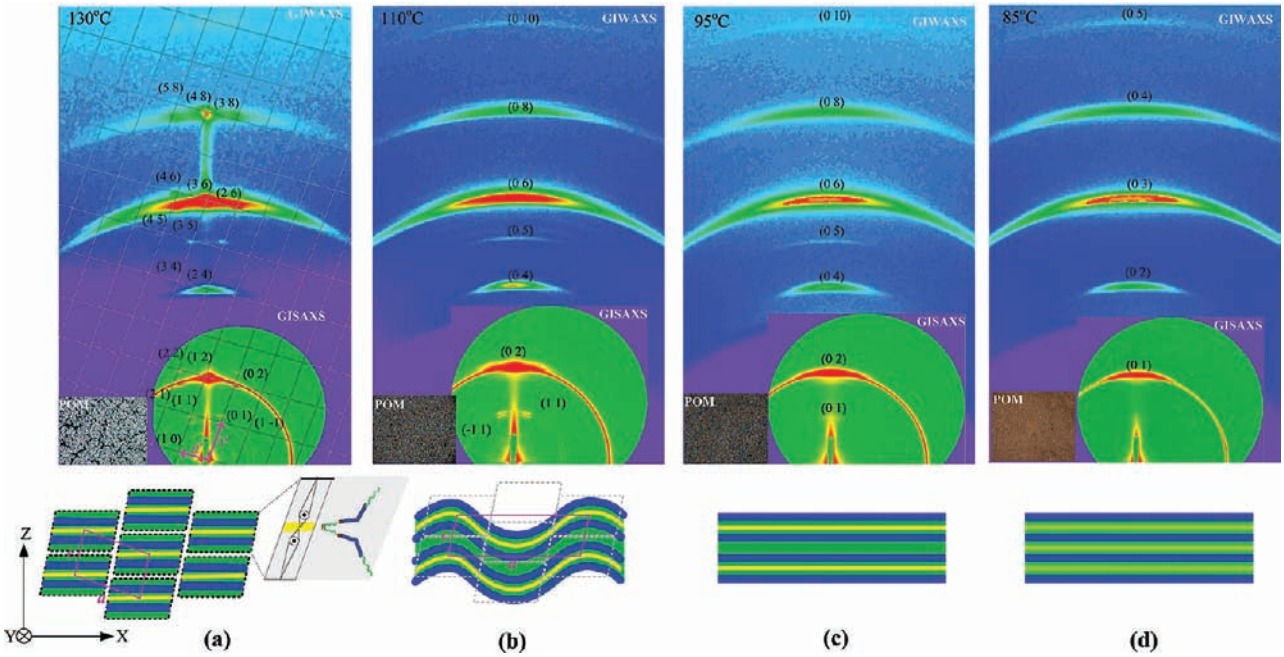

Figure 3. Combined GISAXS and GIWAXS patterns of the surface-aligned sample of the hydrogen-bonded complex **H**−**SiO** at various temperatures: (a) modulated ribbon structure ($Sm\tilde{C}G_2$) at 130 °C; (b) undulated bilayer structure ($USmCG_2$) at 110 °C; (c) bilayer structure ($SmCG_2$) at 95 °C; and (d) monolayer structure (SmCG) at 85 °C. Model: Yellow, green, and blue lines indicate oligosiloxane units, alkyl chains, and aromatic cores, respectively. The light gray part of the inset in (a) shows the molecular organization at a side view along the direction a (right) and front view along the normal direction of the a−c plane (left).

dx.doi.org/10.1021/ja205550b |J. Am. Chem. Soc. 2011, 133, 15674–15685

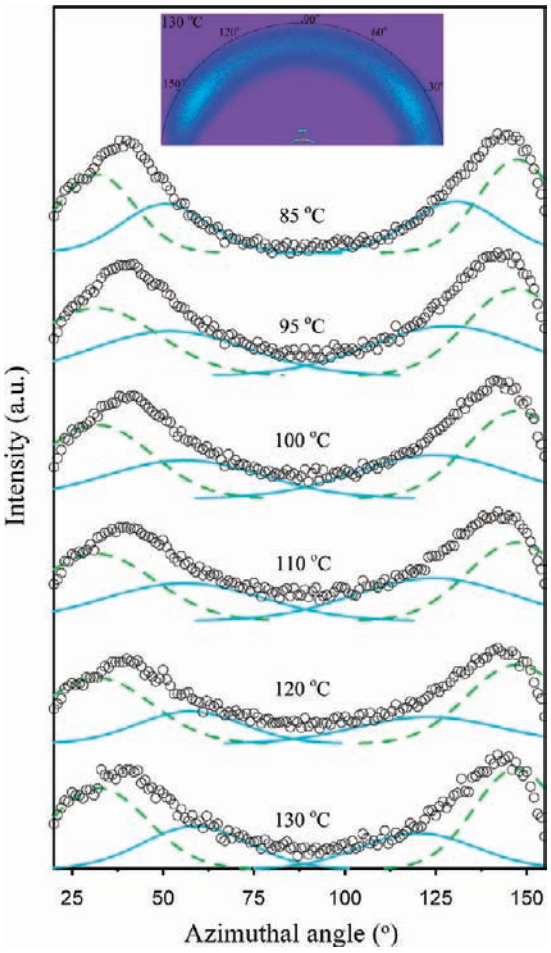

Figure 4. Azimuthal scans of the GIWAXS diffuse halos in the SmCG phases of the hydrogen-bonded complex **H−SiO** at various temperatures, and the zero angle corresponding to the layer normal. The profiles are fitted with two sets of Gaussian curves: the blue curves indicate the decreased mean leaning angles with decreasing temperature from 130 to 85 °C, whereas the green curves indicate a constant mean tilt angle in this temperature range. Inset: 2D-GIWAXS pattern obtained at 130 °C.

monolayer stacking (of a *d*-spacing of 6.2 nm) of the bent-core molecules (Figure 3d). Overall, the X-ray scattering data collected during the cooling process detailed a series of phase transitions of the SmCG-type phase, from modulated bilayers to monolayers ($Sm\tilde{C}G_2$−$USmCG_2$−$SmCG_2$−SmCG), as illustrated by the cartoons in Figure 3; these phase transitions were thermally reversible. These results indicate that the segregation/aggregation of the oligosiloxane terminal groups of the asymmetric hydrogen-bonded complex **H−SiO** associates closely with the formation of the bilayer-based SmCG phase, as was also suggested previously.[14d]

The corresponding GIWAXS profiles in Figure 4 were measured at various temperatures for the SmCG-type phases of the hydrogen-bonded complex **H−SiO**. The corresponding 2D-scattering patterns (for instance, inset of Figure 4 at 130 °C), in general, display an anisotropic diffuse halo ring at $q \approx 13.5$ nm^{-1} (corresponding to a Bragg spacing ~0.47 nm for the packing of the bent-core molecules), with emphases on the two discernible maxima located above the equatorial plane. The locations of the maxima could associate closely with the tilt and leaning angles of the bent-core molecules in the smectic layers of the SmCG-type phase (Figure 5). In addition, a higher value centered at $q \approx 9$ nm^{-1} (or 0.7 nm spacing) is an isotropic halo ring (Figure S4), likely corresponding to a mean distance between the segregated siloxane units as also proposed by Tschierske et al.[14] Furthermore, the azimuthal intensity distributions of the GIWAXS diffuse halos at $q \approx 13.5$ nm^{-1} can be decomposed into two humps (Figure 4) contributed respectively by the tilt and leaning of the hydrogen-bonded complex **H−SiO**, because the surface-aligned sample is 2D powders in which the layers are stacked along the substrate normal but the azimuthal orientation of the layers is random. For the first set, the decomposed humps centered at a constant angle of ca. 31° are insensitive to temperature change, and the angle is close to the calculated tilt angle of 29° based on the measured *d*-spacing and simulated molecular length. For the second set, the hump centers, corresponding to the mean leaning angles, shift slowly from 60° to 50°, as temperature decreased from 130 to 85 °C; the result is consistent with increased hydrogen-bonding strength for a better alignment (smaller leaning) of **H−SiO** along the smectic layer normal. The mean tilt and leaning angles thus decoupled are consistent with those obtained in the case with an electric-field alignment (see next section).

Electric-Field-Oriented SmCG-type Domains. To better illustrate the tilt and leaning angles of the SmCG-type phases of the hydrogen-bonded complex **H−SiO**, we performed in situ SAXS and WAXS measurements under electric fields perpendicular to the X-ray beam, as illustrated in Figure S3. In the corresponding SAXS patterns (Figure 6), all reflections situate along the equatorial direction, and all peak positions are the same as those obtained for the surface aligned sample using GISAXS (Figure 6c), as selectively shown at 95 and 130 °C cases. This result indicates that the bilayer structures were merely oriented along the electric-field direction, as a bookshelf structure, but without local structural changes, such as the tilt angle (as evidenced by the same bilayer *d*-spacing with and without electric field as illustrated in Figure 6c). Furthermore, the GISAXS result reveals a polarized direction of the bilayer in the hydrogen-bonded complex **H−SiO** along the 2D lattice plane, as a $B1_{rev,tilted}$ phase for the modulated bilayer structure ($Sm\tilde{C}G_2$); this finding would frustrate the possibility of a 3D modulated phase proposed by Szydlowska et al.[17] Previously, Jakli et al.[18] suggested that the layer normal of the SmCG phase could be tilted with respect to the direction of the electric field under a large electric field. In this case, we found that the layer normal is only perpendicular to the electric field under a small applied field (0.33 V μm^{-1}) (Figures 6a,b, 7a,b); the small electric field, nevertheless, could effectively align the smectic layer domains of the SmCG-type phases. As noted, the applied small electric field meant to align the layer domains of the SmCG-type phases, rather than individual **H−SiO** molecules by their long or short axes. The successful electric-field alignment can be realized by the largely enhanced peak intensity shown in Figure 6c (corresponding to more oriented SmCG domains). Likely, the electric dipole moments, oriented along the mirror symmetry direction of the back-to-back packed **H−SiO** pairs, are always perpendicular to the smectic layer normal, hence to induce an effective alignment by a small electric field. We emphasize that the applied small electric field did not change the tilt angle of the hydrogen-bonded complex **H−SiO** in the SmCG-type phases, a critical point that allowed the decoupling of the leaning from the tile angle, during the manipulation of the former via temperature.

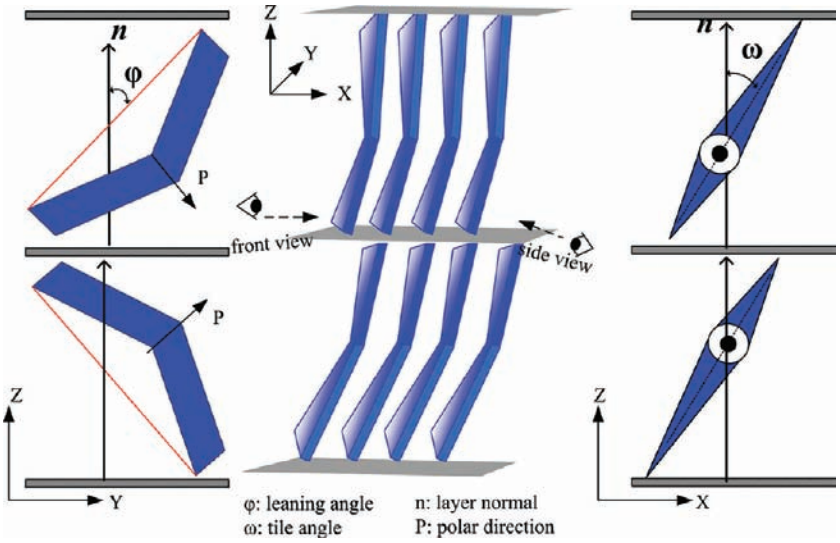

Figure 5. Schematic representation of the orientation of the bent-core molecules in the $SmCG_2$ phase.

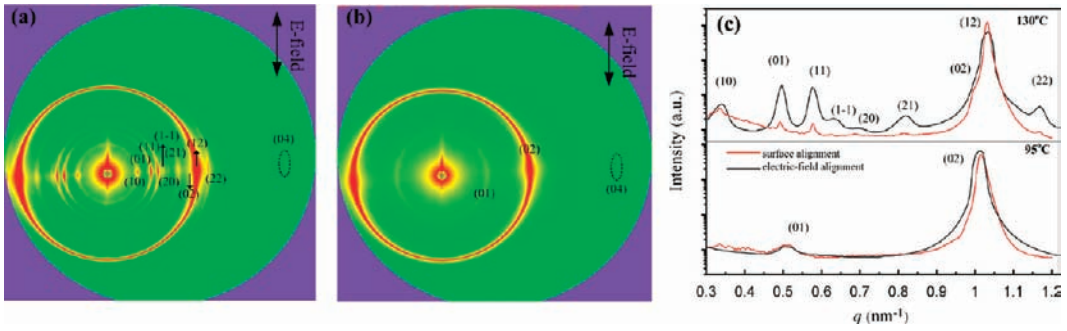

Figure 6. (a,b) SAXS patterns of the electric field-aligned sample of the hydrogen-bonded complex **H−SiO** at (a) 130 and (b) 95 °C. (c) SAXS profiles from (a) and (b) as compared to GISAXS profiles recorded at the same temperatures.

As expected with the applied electric field for better aligned LC domains of the SmCG-type phases, the WAXD patterns recorded at 130 °C (Figure 7a) and 95 °C (Figure 7b) display more clearer four-lobe scattering among the diffuse halo at a q value of 13.5 nm^{-1} (d = 0.47 nm), as compared to the sample in Figure 4 only weakly aligned by a surface coating layer. The WAXS pattern can reveal the leaning angle of the molecules in the SmCG phase in terms of the azimuthal angle distribution of the diffuse halo, if the molecules within the oriented ribbons or layers are perfectly aligned along the electric field. Before turning to a closer examination of the SmCG-type phase transitions, we wish to clarify an additional point regarding how the bending angle of bent-core molecules can be reflected in the azimuthal distribution of an outer diffuse halo. Takanishi et al.[19] verified that the angle between the nearest peaks of a four-lobe diffuse halo is relative to the supplementary angle of the molecular bending angle, as measured using microbeam X-ray scattering (beam size: 3 × 4 μm^2), when the incident beam is normal to the bending plane of the bent-core molecules and the beam size is sufficiently small to detect a single LC grain.

Because we performed the SAXS and WAXS experiments of the electric-field sample cell at a beam diameter of 0.5 mm and a sample thickness of 1 mm, all X-ray data in this study should be average values of the LC polygrains, with the low resolution in the outer diffuse halo resulting in the broad azimuthal distribution of the diffuse halo. Considering our experimental conditions and the bilayer packing structure in the hydrogen-bonded complex **H−SiO**, we believe that the four-lobe diffuse halo is characterized by the projection of the bent-core molecules as a V-shape arrangement along the electric field on the basis of the supposedly neglected molecular bend. The insets of Figure 7a and b present possible bilayer packing structures satisfying the condition for a syn-clinic and anti-leaning $SmCG_2$ phase. Hence, the included angle between the layer normal direction and the nearest one of an azimuthal maximum (Figure 7c) can be assigned as arising from the leaning angle of the bent-core molecules in the SmCG-type phase, if the molecular bending plane were perfectly parallel to the electric field and normal to the incident beam. Although the layer structures were oriented well by the electric field, it was difficult to avoid the rotation of layers around the layer stacking direction in the partial LC domains, due to the nonhomogeneous distribution of the electric field and/or defect domains. With rotation around the columnar axis, the modulated bilayer structure ($Sm\tilde{C}G_2$) lacks the layer rotation effect. As a result, the azimuthal scans of the diffuse halo broadened toward the meridian at the temperature below 110 °C for the phases of undulated bilayer, bilayer, and monolayer structures (Figure 7c). Hence, we need to consider the layer-rotation effect for the temperature below 110 °C. Figure 7c displays the azimuthal scans of the temperature-dependent four-lobe diffuse

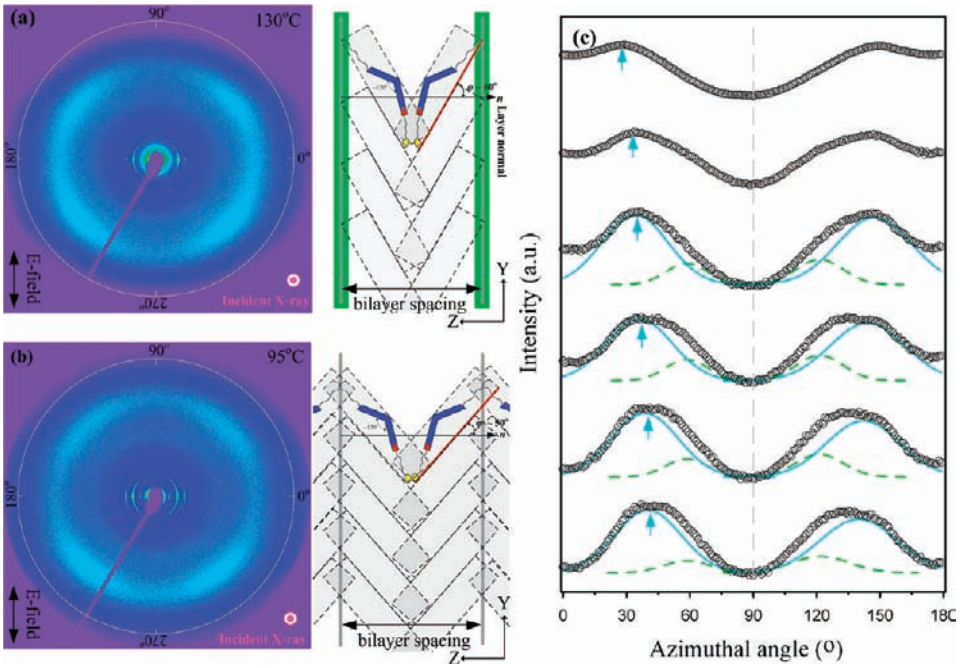

Figure 7. (a,b) WAXS patterns of the electric field-aligned sample and schematic representations of the molecular orientations of the hydrogen-bonded complex **H**−**SiO** at (a) 130 and (b) 95 °C. (c) Azimuthal scans of the diffuse halos at various temperatures, fitted with two sets of Gaussian curves (green and blue curves denoting the contribution from the tilt and leaning angles, respectively).

Table 2. Crystallographic Unit Cell Parameters and Tilt and Leaning Angles of the Hydrogen-Bonded Complex H−SiO at Various Temperatures

	$Sm\tilde{C}G_2$		$USmCG_2$		$SmCG_2$	SmCG
temp (°C)	130	120	110	100	95	85
a (nm)	19.1	18.6				
c (nm)	12.9	12.6	12.3	12.4	12.4	6.2
β	96°	96°				
ω (tilt angle)	31°	31°	31°	31°	30°	30°
φ (leaning angle)	60°	57°	56°	54°	52°	50°

halos from 0 to 180°; the profiles are decomposed into two sets of humps contributed, respectively, by the tilt and leaning angles, following the same procedure as that done previously. The thus extracted leaning angle decreased from approximately 60° to 50° upon decreasing temperature from the modulated bilayer ($Sm\tilde{C}G_2$) at 130 °C to monolayer (SmCG) at 85 °C. On the other hand, the extracted constant tilt angle, ca. 31°, is the same as that extracted without electric fields previously. Table 2 lists the leaning angles thus obtained.

In Table 2, the decrease in the leaning angle from 60° to 50° that accompanied the rich phase transitions reveals that the phase transitions during the cooling process followed the phase sequence Iso−$Sm\tilde{C}G_2$−$USmCG_2$−$SmCG_2$−SmCG in the hydrogen-bonded complex **H**−**SiO**. A large enthalpy change of 14.4 kJ g^{-1} occurred during the Iso−$Sm\tilde{C}G_2$ transition, corresponding to a first-order phase transition; in contrast, the subphase transitions $Sm\tilde{C}G_2$−$USmCG_2$−$SmCG_2$−SmCG, which proceeded without enthalpy formation, may be assigned to a second-order phase transition (Figure S2). These findings suggest that the changes in the leaning angle induced a break in chiral symmetry, leading to the subtle phase transitions. A modulated layer structure of bent-core LCs is usually produced through the formation of a polarization splay.[3,9] In the hydrogen-bonded complex **H**−**SiO**, the modulation can be attributed not so much to the polarization splay as to the larger leaning angle, because the splayed angle of the polar direction between two adjacent molecules was very small (<5°) within the cross section of the bulky ribbons, which comprised approximately 70 molecules. From the mostly unchanged bilayer spacing (or the a-axis length) during the phase transitions, we speculate that the changing of domain wall thickness within the modulated boundaries or the interdigitation of terminal alkyl chains between adjacent bilayers could compensate the changes in bilayer spacing caused by the changes of the leaning angle in the SmCG-type phase transitions (as illustrated in the insets of Figure 7a and b).

In comparison with the SmC phase of the hydrogen-bonded complex **H**−**Alk**, the WAXS pattern recorded under the electric field displayed relatively weaker four-lobe diffuse scattering (Figure 8a). In Figure 8b, the intensity profile obtained from the azimuthal scan of the diffuse halo could also be decomposed into two sets of Gaussian humps, with the hump centered at 90° revealing a zero leaning of **H**−**Alk**, and the other set of humps indicating a tilt angle of about 30°, which is in agreement with that obtained by GIWAXS (Figure 1).

Structural Effects of Hydrogen Bonding and Siloxane Groups on the SmCG Phases. Unlike the hydrogen-bonded complex **H**−**Alk** and covalent-bonded compound **C**−**SiO**, the hydrogen-bonded complex **H**−**SiO**, featuring both hydrogen bonds and branched siloxane units, was the only system exhibiting the bilayer structure with complicated SmCG-type phase transitions. This situation seems to imply that interplay between the stability of the hydrogen bonds and the microsegregation of the siloxane units has an important effect on the molecular packing of the bilayer structure. It is necessary, at this point, for us to clarify the relationship between the SmCG-type phase

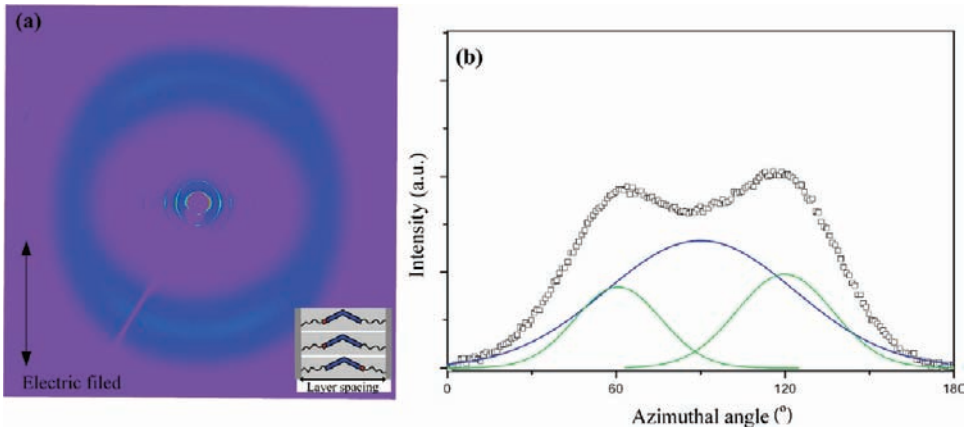

Figure 8. (a) WAXS pattern and (b) azimuthal scan of the diffuse halos (green curves denoting the contribution from the layer rotation effect; blue curves indicating the molecular orientation) of the hydrogen-bonded complex **H−Alk** at 110 °C under an electric field.

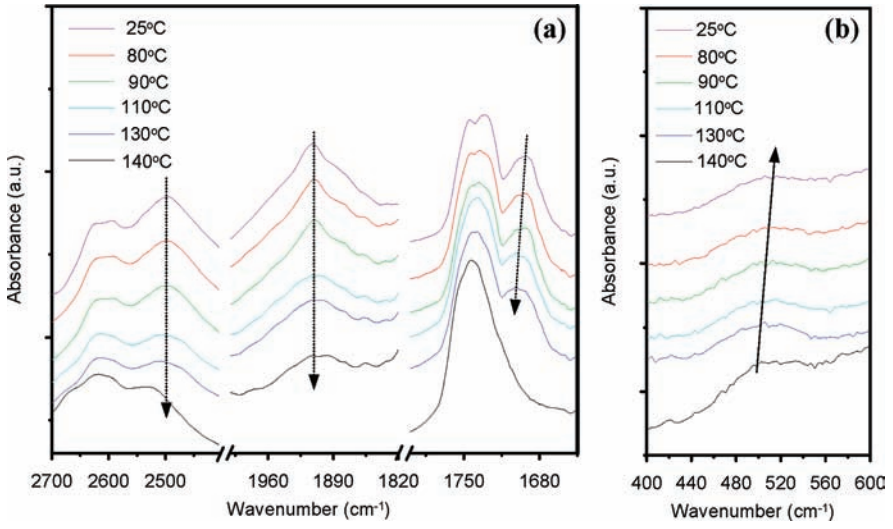

Figure 9. (a) FTIR spectra of the hydrogen-bonded complex **H−SiO** at various temperatures. Two O−H bands appear at 2500 and 1940 cm^{-1}. The C═O band, influenced by the formation of hydrogen bonds between the pyridyl and carboxylic acid groups, appears in the range 1780−1640 cm^{-1}. (b) Temperature-dependent Raman spectra of the characteristic peaks for Si−O−Si symmetric stretching bands.

transitions of the hydrogen-bonded complex **H−SiO** in terms of the stability of the hydrogen bonds and the microsegregation. Figure 9a and b presents FTIR and Raman spectra, respectively, recorded at various temperatures corresponding to the Iso (140 °C), $Sm\tilde{C}G_2$ (130 °C), $SmCG_2$ (90 °C), SmCG (80 °C), and crystalline (RT) phases of the hydrogen-bonded complex **H−SiO**. The signals for the O−H bonds appeared at 1940 and 2500 cm^{-1} and the C═O band shifted from 1687 to 1693 cm^{-1}, confirming the formation of hydrogen bonds between the carboxylic acid units of **3SiA** and the pyridyl groups of **VPy**.[20] When the system approached the isotropic phase, weakening of the hydrogen bonds occurred: the signals of the O−H bonds weakened and broadened, and the C═O band shifted to higher wavenumber. On the other hand, the characteristic peak at 500 cm^{-1} for Si−O−Si symmetric stretching in the Raman spectrum[21] shifted slightly to higher wavenumber at the higher temperature, presumably because of relatively enhanced microsegregation of the siloxane units upon weakening of the hydrogen bonds.

Both the FTIR and the Raman spectral data suggest that the existence of the hydrogen bonds strongly affected the molecular orientation of hydrogen-bonded complex **H−SiO**. Dependence of phase behavior on hydrogen bonds has been observed in other supramolecular LC systems.[20] On the basis of the FTIR and Raman spectra, we suggest that the balance between the hydrogen bonding and segregation of the siloxane units resulted in the changes of the leaning angles in the SmCG-type phase transitions of **H−SiO**. Correspondingly, measured FTIR and Raman spectra for compounds **C−SiO** and **H−Alk** (Figures S5 and S6) support the hydrogen bonding and influence on the fine structural changes of the SmCG phase in the hydrogen-bonded complex **H−SiO**. At high temperatures, hydrogen bonding was weakened, and a stronger segregation of siloxane units resulted in larger leaning angles. A larger leaning angle would cause the molecular mass center to deviate substantially from the central position of the layer, and hence to induce the modulation or undulation layers ($Sm\tilde{C}G_2$ and $USmCG_2$). At lower temperatures, the stronger hydrogen-bonding strength suppresses the leaning and leads to the transition toward the monolayer SmCG phase. The transformation from the bilayer $SmCG_2$ to monolayer

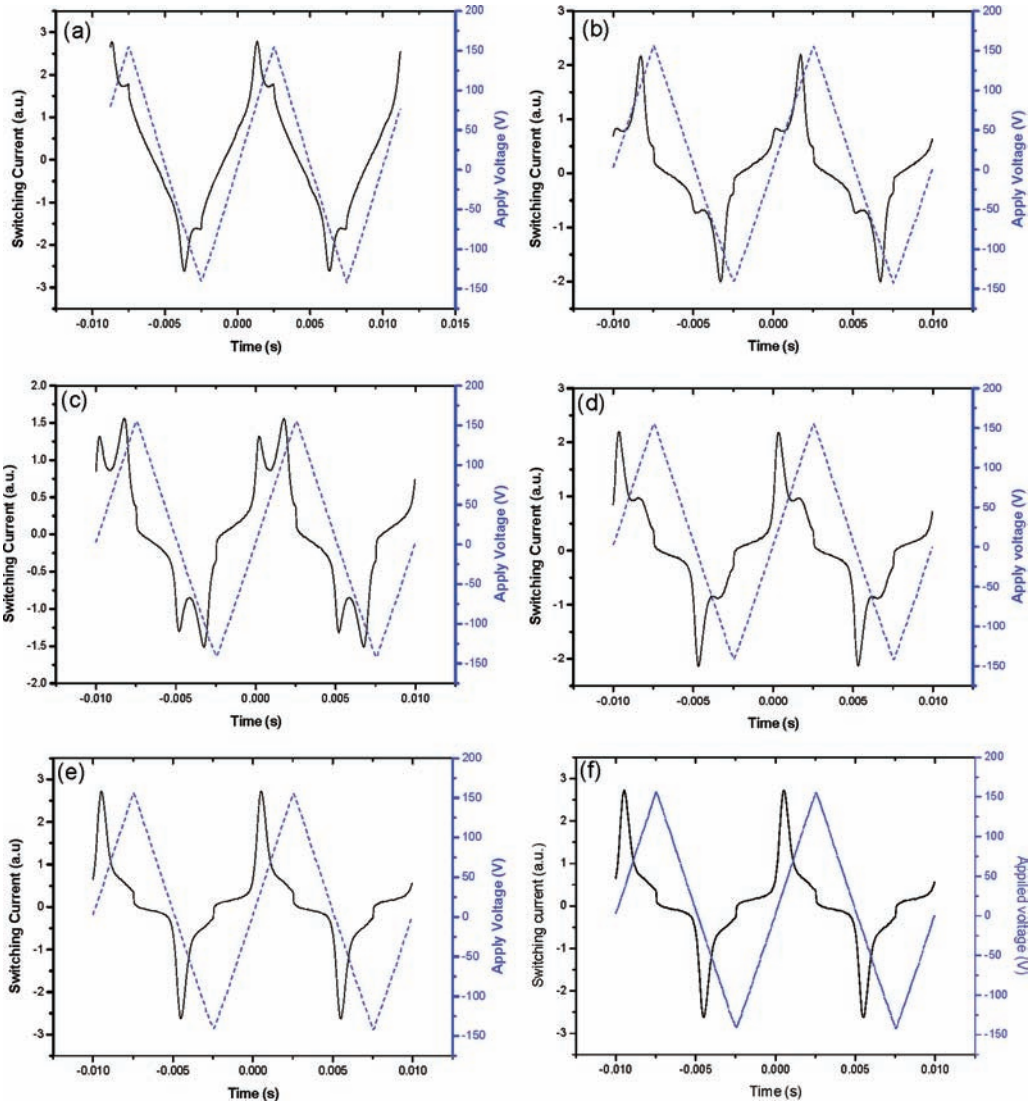

Figure 10. Switching current response curves of the hydrogen-bonded complex **H−SiO** under applied triangular waves (V_{PP} = 300 V; f = 100 Hz; in parallel rubbing cells: thickness, 7.5 μm) at (a) 130, (b) 113, (c) 103, (d) 97, (e) 95, and (f) 85 °C.

SmCG phase at low temperatures indicates a favorable monolayer packing of the hydrogen-bonded complex **H−SiO**.

Electro-optical Properties. Combining the switching current responses with the XRD data obtained at various temperatures facilitates the characterization of the mesomorphic properties of these bent-core LCs. Thus, to prove the polar switching properties of the three analogous compounds (**H−SiO**, **C−SiO**, and **H−Alk**), we employed the triangular wave technique[22] to measure the switching current behavior (including verifications of ferroelectricity, antiferroelectricity, and spontaneous polarization by repolarization current peaks) in parallel rubbing cells having a thickness of 7.5 μm. For the hydrogen-bonded complex **H−SiO**, three modes appeared for the polar switching currents during the cooling process.[23] In the highest-temperature LC phase range (identified as the modulated bilayer structure in the X-ray measurements), a single repolarization current peak was observed at 132 °C during the half period of the applied triangle voltage (Figure 10a); this clearly indicates a ferroelectric switching process. In addition, the modified triangular wave could also verify the ferroelectric switching process further (see Figure S7a). Consequently, the $Sm\tilde{C}G_2P_F$ phase, as the highest-temperature mesophase, of the hydrogen-bonded complex **H−SiO** possessed a general tilted bilayer modulated smectic phase with a longer modulation periodicity in the oblique lattice (as determined through X-ray measurements) and ferroelectricity (as determined though switching current measurements). Figure 11 presents POM photos images of the circular domains in all of the mesophases (i.e., the SmCG phases) of the hydrogen-bonded complex **H−SiO** under dc electric fields of +50 and 0 V. The circular domains of the mosaic-like texture in the hydrogen-bonded complex **H−SiO** at 130 °C, typical for the $Sm\tilde{C}G_2P_F$ phase, did not alter upon changing of the applied voltage because of an unfavorable cone-like rotation in the modulations (Figure 11a and b). When we decreased the temperature of the hydrogen-bonded complex **H−SiO** gradually to 113 °C, two repolarization peaks steadily appeared (Figure 10b). Furthermore, the initial peak intensity of the $Sm\tilde{C}G_2P_F$ phase decreased and the newly evolved peak increased its intensity upon decreasing temperature (to 103 °C in Figure 10c and to 97 °C in Figure 10d). Therefore, the switching current behavior, with two

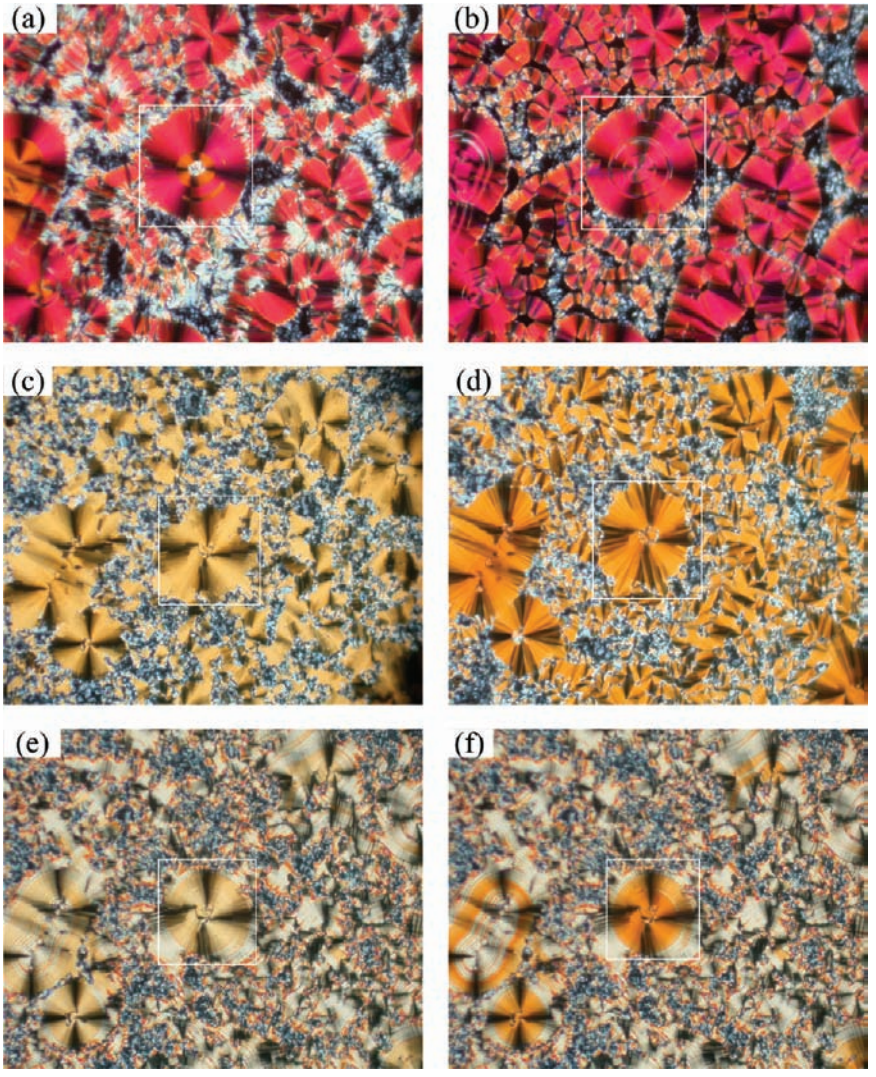

Figure 11. Circular domains of the hydrogen-bonded complex **H**−**SiO** measured under various dc electric fields upon cooling (in parallel rubbing cells: thickness, 7.5 μm): (a) +50 V at 130 °C; (b) 0 V at 130 °C; (c) +50 V at 105 °C; (d) 0 V at 105 °C; (e) +50 V at 85 °C; and (f) 0 V at 85 °C.

repolarization peaks present in the range 113−97 °C, confirmed an antiferroelectric switching process. As a result, the USmCG_2-P_A phase, as the second second-highest-temperature mesophase, of the hydrogen-bonded complex **H**−**SiO** possessed a general tilted bilayer undulated smectic phase (as determined through X-ray measurements) and antiferroelectricity (as determined through switching current measurements). The nonvariations of the circular domains were preserved under dc electric fields of +50 and 0 V (see Figure 11c and d),[24] most likely the result of a modulated or an undulated smectic phase possessing a long undulation or modulation periodicity. Further cooling to 95 and 85 °C by applying a triangular wave (see Figure 10e and f, respectively) and a modified triangular wave (see Figure S7b) resulted in only one sharp peak for the hydrogen-bonded complex **H**−**SiO**, indicating a ferroelectric switching process. Accordingly, the SmCG_2P_F and SmCGP_F phases, as the lowest-temperature mesophases, of the hydrogen-bonded complex **H**−**SiO** possessed respectively general tilted bilayer and monolayer smectic phases (as determined through the X-ray measurements) as well as ferroelectricity (as determined through switching current measurements). The extinction crosses were all parallel to the polarizer and analyzer (Figure 11e and f), indicating an overall anti-clinic organization of the molecules.[25] In general, the presence of the circular domains grown under dc fields of +50 V indicates that none of the variations of the extinction crosses were caused by the molecular rotations around the long axis[26] in the studied temperature range, most likely because of the steric effects induced by the siloxane units (rather than the aromatic core) of **H**−**SiO**. Therefore, the branched siloxane terminus of **H**−**SiO** offered sufficient free space for rapid reorientation of the molecules around their long axes, thereby restricting the molecular rotation on a cone. Along with the smectic layered structure confirmed by the X-ray measurements, the antiferroelectric formation suggested by the two-peak switching current response in Figure 12a proves that the hydrogen-bonded complex **H**−**Alk** possessed the SmCP_A phase.[27] On the other hand, the SmCP_F structure (i.e., the B2 phase) of the covalent-bonded compound **C**−**SiO** was characterized by a one-peak switching current response in Figures 12b and S7c, Sm$\tilde{C}G_2$, and a smectic layered structure obtained from the X-ray measurements. POM textures for **H**−**Alk** at 110 °C (V_{pp} = 300 V; f = 100 Hz) and **C**−**SiO** at 150 °C (V_{pp} = 100 V; f = 100 Hz) were

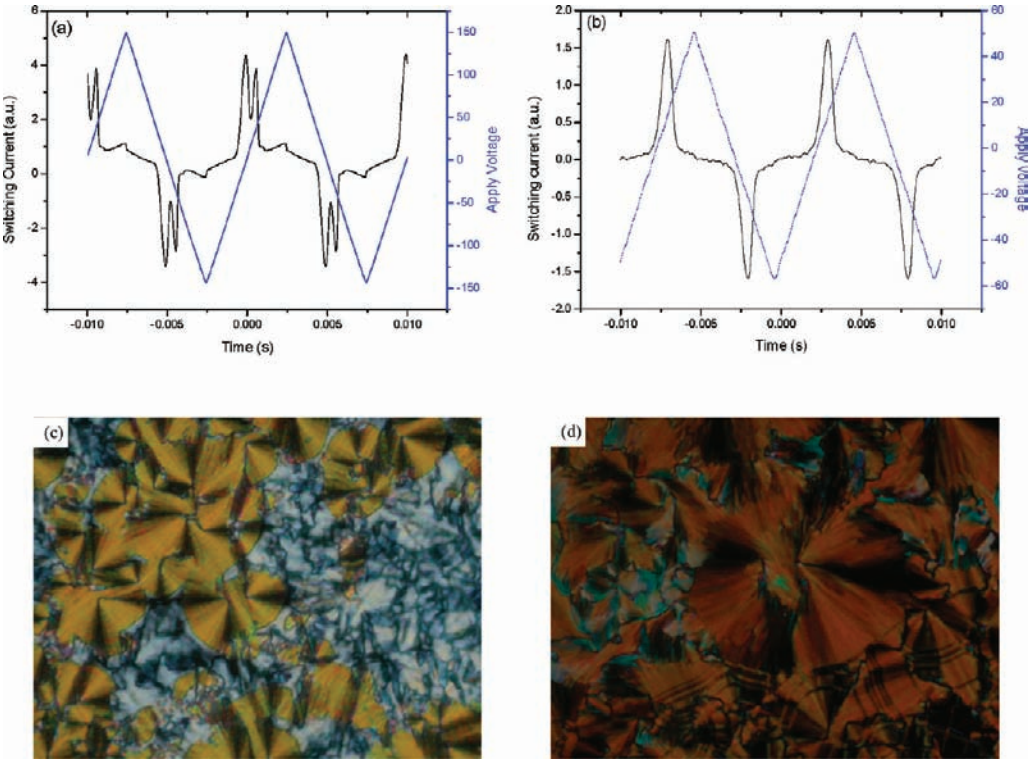

Figure 12. Switching current response curves under applied triangular waves (in parallel rubbing cells: thickness, 7.5 μm) for the (a) hydrogen-bonded complex **H**−**Alk** at 110 °C (V_{pp} = 300 V; f = 100 Hz) and (b) covalent-bonded compound **C**−**SiO** at 150 °C (V_{pp} = 100 V; f = 100 Hz); POM textures of the corresponding switching current measurements for (c) **H**−**Alk** at 110 °C (V_{pp} = 300 V; f = 100 Hz) and **C**−**SiO** at 150 °C (V_{pp} = 100 V; f = 100 Hz).

also shown in Figure 12c and d. With these results, we have demonstrated the interplay between the hydrogen bonding and segregation of siloxane terminal groups in the SmCG phases of the three mutually contrasting bent-core LCs of **H**−**SiO**, **H**−**Alk**, and **C**−**SiO**.

CONCLUSIONS

In this study, we investigated the local molecular packing within the mesophase structures of three analogous bent-core molecules, the hydrogen-bonded complex and the covalent-bonded compound with branched siloxane units (**H**−**SiO** and **C**−**SiO**, respectively) and the hydrogen-bonded complex lacking siloxane units (**H**−**Alk**). Whereas the hydrogen-bonded complex **H**−**Alk** and the covalent-bonded compound **C**−**SiO** exhibited $SmCP_A$ and $SmCP_F$ phases, respectively, the hydrogen-bonded complex **H**−**SiO** exhibited various novel SmCG-type phases. The leaning angles, relative to the molecular arrangements, in the $SmCG_2$-type phases resulted in wide-angle diffuse halos evident though in situ X-ray scattering under dc electric fields. This approach is a simple and direct method of probing SmCG-type phases when the differences between tilt and leaning angles are sufficiently large to be recognized by the azimuthal angle distributions of outer diffuse halos. For the hydrogen-bonded complex **H**−**SiO**, modulated ribbons merged gradually into a monolayer, resulting in the phase sequence $SmCG_2P_F$−$USmCG_2P_A$−$SmCG_2P_F$−$SmCGP_F$ during the cooling process. We also determined the SmCG-type phase transitions of the hydrogen-bonded complex **H**−**SiO** as a function of temperature in terms of its leaning angles, which were related to the competition between the hydrogen-bonded linkages and the microsegregation of the terminal siloxane units. Therefore, for the hydrogen-bonded complex **H**−**SiO**, the effects of the hydrogen bonding and branched siloxane unit induced the bent-core LC molecules to undergo self-assembly to form a series of highly ordered 2D structures. Supramolecular design with hydrogen bonds and terminal siloxane units is interesting not only from theoretical viewpoints but also for the potential applications of structurally designed LC templates.

ASSOCIATED CONTENT

Supporting Information. Complete refs 3 and 16; and detailed synthesized schemes, figures of FTIR, Raman, DSC, and SAXS, WAXS setup under an electric field, and the modified triangle method. This material is available free of charge via the Internet at http://pubs.acs.org.

AUTHOR INFORMATION

Corresponding Author
weitsung@nsrrc.org.tw; linhc@mail.nctu.edu.tw

ACKNOWLEDGMENT

We thank Dr. C. J. Su for help with the SAXS/GISAXS measurements and the National Science Council of Taiwan (ROC) for financial support through NSC97-2113-M-009-006-MY2 and NSC99-2218-E-213-001-MY3.

REFERENCES

(1) Niori, T.; Sekine, T.; Watanabe, J.; Furukawa, T.; Takezoe, H. *J. Mater. Chem.* **1996**, *6*, 1231–1233.

(2) (a) Reddy, R. A.; Tschierske, C. *J. Mater. Chem.* **2006**, *16*, 907–961 and references cited therein. (b) Pelzl, G.; Diele, S.; Weissflog, W. *Adv. Mater.* **1999**, *11*, 707–724. (c) Takezoe, H.; Takanishi, Y. *Jpn. J. Appl. Phys.* **2006**, *45*, 597–625. (d) Lee, S. K.; Heo, S.; Lee, J. G.; Kang, K. T.; Kumazawa, K.; Nishida, K.; Shimbo, Y.; Takanishi, Y.; Watanabe, J.; Doi, T.; Takahashi, T.; Takezoe, H. *J. Am. Chem. Soc.* **2007**, *17*, -11058–11091. (e) Otani, T.; Araoka, F.; Ishikawa, K.; Takezoe, H. *J. Am. Chem. Soc.* **2009**, *131*, 12368–12372. (f) Chen, D.; Maclennan, J. E.; Shao, R.; Yoon, D. K.; Wang, H.; Korblova, E.; Walba, D. M.; Glaser, M. A.; Clark, N. A. *J. Am. Chem. Soc.* **2011**, DOI: 10.1021/ja203522x.

(3) Coleman, D. A.; et al. *Science* **2003**, *301*, 1204–1211.

(4) (a) Mieczkowski, J.; Gomola, K.; Koseska, J.; Pociecha, D.; Szydlowska, J.; Gorecka, E. *J. Mater. Chem.* **2003**, *13*, 2132–2137. (b) Reddy, R. A.; Sadashiva, B. K.; Raghunathan, V. A. *Chem. Mater.* **2004**, *16*, 4050–4062. (c) Bedel, J. P.; Rouillon, J. C.; Marcerou, J. P.; Nguyen, H. T.; Achard, M. F. *Phys. Rev. E* **2004**, *69*, 061702. (d) Murthy, H. N. S.; Sadashiva, B. K. *J. Mater. Chem.* **2004**, *14*, 2813–2821. (e) Reddy, R. A.; Sadashiva, B. K.; Baumeister, U. *J. Mater. Chem.* **2005**, *15*, 3303–3316.

(5) (a) Walba, D. W.; Körblova, E.; Shao, R.; Maclennan, J. E.; Link, D. R.; Glaser, M. A.; Clark, N. A. *Science* **2000**, *288*, 2181–2184. (b) Reddy, R. A.; Raghunathan, V. A.; Sadashiva, B. K. *Chem. Mater.* **2005**, *17*, 274–283. (c) Weissflog, W.; Naumann, G.; Kosata, B.; Schroder, M. W.; Eremin, A.; Diele, S.; Vakhovskaya, Z.; Kresse, H.; Friedemann, R.; Ramakrishnan, S. A.; Pelzl, G. *J. Mater. Chem.* **2005**, *15*, 4328–4337. (d) Umadevi, S.; Sadashiva, B. K.; Murthy, H. N. S.; Raghunathan, V. A. *Soft Matter* **2006**, *2*, 210–214.

(6) de Gennes, P. G. *The Physics of Liquid Crystals*; Clarendon Press: Oxford, 1975.

(7) Brand, H. R.; Cladis, P. E.; Pleiner, H. *Eur. Phys. J. B* **1998**, *6*, 347–353.

(8) (a) Bedel, J. P.; Rouillon, J. C.; Marcerou, J. P.; Achard, M. F. *Pramana, J. Phys.* **2003**, *61*, 395–404. (b) Bedel, J. P.; Rouillon, J. C.; Marcerou, J. P.; Nguyen, H. T.; Achard, M. F. *Phys. Rev. E* **2004**, *69*, 061702.

(9) (a) Pociecha., D.; Vaupotič, N.; Gorecka, E.; J. Mieczkowski, J.; Gomola, K. *J. Mater. Chem.* **2008**, *18*, 881–885. (b) Gorecka, E.; Pociecha, D.; Vaupotič, N.; Čepič, M.; Gomola, K.; Mieczkowskia, J. *J. Mater. Chem.* **2008**, *18*, 3044–3049. (c) Vaupotič, N.; Pociecha, D.; Čepič, M.; Gomola, K.; Mieczkowskia, J.; Gorecka, E. *Soft Matter* **2009**, *5*, 2281–2285.

(10) Rey, A. D. *Soft Matter* **2010**, *6*, 3402–3429.

(11) (a) Stupp, S. I.; Son, S.; Lin, H. C.; Li, L. S. *Science* **1993**, *259*, 59–63. (b) Kato, T.; Mizoshita, N.; Kishimoto, K. *Angew. Chem., Int. Ed.* **2006**, *45*, 38–68. (c) Vera, F.; Tejedor, R. M.; Romero, P.; Barber, J.; Ros, M. B.; Serrano, J. L.; Sierra, T. *Angew. Chem., Int. Ed.* **2007**, *46*, 1873–1877.

(12) (a) Gimeno, N.; Ros, M. B.; Serrano, J. L.; de la Fuente, M. R. *Angew. Chem., Int. Ed.* **2004**, *43*, 5235–5238. (b) Gimeno, N.; Ros, M. B.; Serrano, J. L. *Chem. Mater.* **2008**, *20*, 1262–1271. (c) Perez, A.; Gimeno, N.; Vera, F.; Ros, M. B.; Serrano, J. L.; de la Fuente, M. R. *Eur. J. Org. Chem.* **2008**, *5*, 826–833.

(13) (a) Wang, L. Y.; Chiang, I. H.; Yang, P. J.; Li, W. S.; Chao, I. T.; Lin, H. C. *J. Phys. Chem. B* **2009**, *113*, 14648–14660. (b) Yang, P. J.; Wang, L. Y.; Tang, C. Y.; Lin, H. C. *J. Polym. Sci., Part A: Polym. Chem.* **2010**, *48*, 764–774. (c) Wang, L. Y.; Tsai, H. Y.; Lin, H. C. *Macromolecules* **2010**, *43*, 1277–1288.

(14) (a) Dantlgraber, G.; Eremin, A.; Diele, S.; Hauser, A.; Kress, H.; Pelzl, G.; Tschierske, C. *Angew. Chem., Int. Ed.* **2002**, *41*, 2408–2412. (b) Keith, C.; Reddy, R. A.; Baumeister, U.; Tschierske, C. *J. Am. Chem. Soc.* **2004**, *126*, 14312–14313. (c) Keith, C.; Reddy, R. A.; Hauser, A.; Baumeister, U.; Tschierske, C. *J. Am. Chem. Soc.* **2006**, *16*, 3051–3066. (d) Keith, C.; Dantgraber, G.; Reddy, R. A.; Baumeister, U.; Prehm, M.; Hahn, H.; Lang, H.; Tschierske, C. *J. Mater. Chem.* **2007**, *17*, 3796–3805.

(15) Mehl, G. H.; Goodby, J. W. *Chem. Ber.* **1996**, *129*, 521–525.

(16) Jeng, U. S.; et al. *J. Appl. Crystallogr.* **2010**, *43*, 110–121.

(17) Szydlowska, J.; Mieczkowskia, J.; Matraszek, J.; Bruce, D. W.; Gorecka, E.; Pociecha, D.; Guillon, D. *Phys. Rev. E* **2003**, *67*, 031702.

(18) (a) Jákli, A.; Krüerke, D.; Sawade, H.; Heppke, G. *Phys. Rev. Lett.* **2001**, *86*, 5715–5718. (b) Rauch, S.; Bault, P.; Sawade, H.; Heppke, G.; Nair, G. G.; Jákli, A. *Phys. Rev. E* **2002**, *66*, 021706. (c) Jákli, A.; Nair, G. G.; Sawade, H.; Heppke, G. *Liq. Cryst.* **2003**, *30*, 265–271.

(19) Takanishi, Y.; Toshimitsu, M.; Nakata, M.; Takada, N.; Izumi, T.; Ishikawa, K.; Takezoe, H.; Watanabe, J.; Takahashi, Y.; Lida, A. *Phys. Rev. E* **2006**, *74*, 051703.

(20) Kato, T.; Fréchet, J. M. J.; Wilson, P. G.; Takeshi Saito, T.; Uryu, T.; Fujishima, A.; Jin, C.; Kaneuchi, F. *Chem. Mater.* **1993**, *5*, 1094–1100.

(21) Julián, B.; Gervais, C.; Cordoncillo, E.; Escribano, P.; Babonneau, F.; Sanchez, C. *Chem. Mater.* **2003**, *15*, 3026–3034.

(22) Miyasato, K.; Abe, S.; Takazoe, H.; Fukuda, A.; Kuze, E. *Jpn. J. Appl. Phys.* **1983**, *22*, L661.

(23) Keith, C.; Dantlgraber, G.; Reddy, R. A.; Baumeister, U.; Tschierske, C. *Chem. Mater.* **2007**, 694–710.

(24) Geese, K.; Prehm, M.; Tschierske, C. *J. Mater. Chem.* **2010**, *20*, 9658–9665.

(25) (a) Keith, C.; Reddy, R. A.; Baumeister, U.; Kresse, H.; Chao, J. L.; Hahn, H.; Lang, H.; Tschierske, C. *Chem.-Eur. J.* **2007**, *13*, 2556–2577. (b) Zhang, Y.; Baumeister, U.; Tschierske, C.; O'Callaghan, M. J.; Walker, C. *Chem. Mater.* **2010**, *22*, 2869–2884.

(26) Gorecka, E.; Vaupotic, N.; Pociecha, D.; Cepic, M.; Mieczkowski, J. *ChemPhysChem* **2005**, *6*, 1087–1093.

(27) Zenyoji, M.; Takanishi, Y.; Ishikawa, K.; Thisayukta, J.; Watanabe, J.; Takezoe, H. *J. Mater. Chem.* **1999**, *9*, 2775–2778.